Journal of Drug Delivery Science and Technology 52 (2019) 586–596

Contents lists available at ScienceDirect

Journal of Drug Delivery Science and Technology

journal homepage: www.elsevier.com/locate/jddst

Dual-functional melatonin releasing device loaded with PLGA microparticles and cyclodextrin inclusion complex for osteosarcoma therapy

Damla Çetin Altındal, Menemşe Gümüşderelioğlu*

Hacettepe University, Chemical Engineering Department, 06800, Beytepe, Ankara, Turkey

ARTICLE INFO

Keywords:
Melatonin
Bone tissue engineering
Controlled release
Osteosarcoma
Inclusion complex

ABSTRACT

The aim of this study is to develop a scaffold-based device in which both osteoinductive and anticarcinogenic properties of melatonin can be combined for osteosarcoma therapy. While a high melatonin concentration and fast release are needed to achieve an anticancer effect, a low melatonin concentration and long-term release are necessary for bone regeneration. Long-term controlled release of melatonin was provided by the incorporation of melatonin-loaded poly(lactic-co-glycolic acid) (PLGA) microparticles into the chitosan/hydroxyapatite (chitosan/HAp) scaffolds. This system showed a biphasic melatonin release-pattern with a burst release within 24 h, and then, a sustained release for 40 days that resulted into ~40–70 μM concentration. Preosteoblastic MC3T3-E1 cells were cultured on this 3D device, and released melatonin caused increase in the expressions of osteogenic differentiation markers. For the inhibition of MG-63 human osteosarcoma cells, a melatonin/2-hydroxypropyl-β-cyclodextrin (HPβCD) inclusion complex was prepared by microwave technology to load a high amount of melatonin and provide fast release. Melatonin/HPβCD inclusion complex was incorporated into the chitosan/HAp scaffolds and loaded melatonin was rapidly released within 5 h and inhibited the proliferation of MG-63 cells in the G_0/G_1 phase. In conclusion, this melatonin-releasing scaffold-based device including melatonin-loaded PLGA microparticles and melatonin/HPβCD inclusion complex can be considered as a promising system for osteosarcoma therapy.

1. Introduction

Melatonin is one of the hormones that play an important role in bone regeneration *in vitro*, bone formation *in vivo* and prevents the development of scoliosis [1,2]. Several studies have demonstrated that nano/micromolar concentrations of melatonin have a positive effect on the recruitment and differentiation of preosteoblast/osteoblast/osteoblast-like cells [1,3–5]. Further, the use of melatonin alone, or in combination with other growth factors in positions where bone implants are placed in the body, provides positive results. This is due to its new bone formation capacity and the ability to increase osseointegration [6]. Sustained release of melatonin over a prolonged time can have better effects on the bone repair process than its direct injection to the site of injury or the direct loading onto the scaffolds, each of which may not have the appropriate effect due to drug exposure being only in the early stages [2,7]. Although melatonin has several advantages in bone regeneration, its sensitivity to oxidation and light and its short half-life (30–60 min) together, constitute a major problem in achieving adequate bioavailability [8]. In order to increase the stability of melatonin molecule, polymeric carrier systems can be used.

Melatonin is also known to have antioxidant, antiproliferative, and oncostatic properties [9]. Several studies have provided evidence that melatonin may significantly inhibit the growth of various types of tumors, such as breast, ovary, endometrium, prostate, liver, and bone [9–11]. Melatonin also reduces the side effects of chemotherapeutic drugs and promotes their efficiency on tumor reduction [12]. In addition, melatonin restrains the uptake of linoleic acid, which is a tumor growth factor [13] and inhibits telomerase activity of cancer cells [14]. Osteosarcoma is the most common primary malignancy of bone, and is treated with chemotherapy after surgical removal of the tumor site. However, chemotherapy is a very challenging process and affects the whole body, not just the cancerous tissue. For this reason, tumor-specific therapies with fewer side effects have been developed. However, for a tumor-specific therapy, melatonin concentration must be selected carefully. While nano/micromolar (1 nM–10 μM) melatonin concentrations had no effect on the morphology or growth of human osteosarcoma MG-63 cells [15], millimolar concentrations of melatonin (~4–10 mM) inhibited the proliferation of MG-63 cells and significantly induced cell cycle arrest [11].

Cyclodextrins (CDs) are cyclic oligosaccharides composed of (α-

* Corresponding author.
E-mail addresses: menemse@hacettepe.edu.tr, menemse@gmail.com (M. Gümüşderelioğlu).

https://doi.org/10.1016/j.jddst.2019.05.027
Received 22 February 2019; Received in revised form 12 May 2019; Accepted 13 May 2019
Available online 15 May 2019
1773-2247/

1,4)-linked D-glycopyranose molecules with a hydroxyl group on their outer surface and a hydrophobic cavity in the center [16,17]. The inclusion complex is formed by the entrance of a guest molecule into the inner cavity of the host CD structure [18]. Although melatonin has significant properties, its usage is limited due to its low water solubility. The amphiphilic structure of melatonin makes it suitable for the formation of inclusion complexes by insertion into the rigid hydrophobic cavity of CDs [19]. Therefore, melatonin-cyclodextrin inclusion complexes can increase melatonin solubility and thus improve its utilization.

By taking into account the related literature, we decided to develop an implantable 3D-scaffold-based system in which the osteoinductive and anticarcinogenic properties of melatonin can be combined. The proliferative and osteoinductive effect of the melatonin on pre-osteoblastic cells and the inhibitory effect on the osteosarcoma cells were realized by incorporating two different carrier systems into the 3D porous tissue scaffolds to achieve melatonin release in the desired doses at the desired times. Melatonin was loaded into the PLGA microparticles to support bone regeneration with sustained release. For the inhibition of osteosarcoma cells, a melatonin/CD inclusion complex was prepared to release high amount of melatonin rapidly. These two types of melatonin-carrying and -releasing systems were incorporated into porous chitosan/HAp scaffolds. The effectiveness of these scaffold-based devices was investigated by *in vitro* cell cultures.

2. Materials and methods

2.1. Materials

Melatonin (MW: 232.28 g/gmol) and poly(D,L-lactide-co-glycolide) (PLGA) (MW: 40,000–75,000 Da) with 50:50 copolymer ratio of D,L-lactide to glycolide were obtained from Sigma (Germany). Polyvinyl alcohol (PVA; MW: 89,000–98,000 g/gmol) as surfactant and dichloromethane (DCM) as organic solvent were obtained from Sigma-Aldrich (Germany). Chitosan (77%–85% degree of deacetylation (DD); MW: 190,000–310,000 Da) and acetic acid were purchased from Sigma (Germany) and Riedel de Haen (Germany), respectively. Hydroxyapatite (HAp) beads with particle size of 45–80 μm were obtained from Science Application Industries (France). Sodium carbonate, used for neutralization of the scaffolds, and 2-hydroxypropyl-β-cyclodextrin (HPβCD) (MW ~1460 g/mol) were both obtained from Sigma-Aldrich (Germany). In cell culture studies, fetal bovine serum (FBS), penicillin-streptomycin, 1, 3-(4,5-dimethylthiazol-2-yl)-diphenyltetrazolium bromide (MTT), β-glycerol phosphate, L-ascorbic acid and hexamethyldisilazane (HMDS) were purchased from Sigma-Aldrich (Germany). Minimum essential medium-α (α-MEM) and Dulbecco's modified Eagle's medium (DMEM) were obtained from Biowest (USA).

2.2. Preparation of melatonin-loaded PLGA microparticles

Melatonin-loaded PLGA microparticles were prepared by the single emulsion-solvent evaporation method described previously [20]. Briefly, 0.1 g of PLGA and 20% (w/w) of melatonin with respect to polymer were dissolved in 5 mL of DCM to obtain the organic phase. In addition, 0.2% (w/v) melatonin was added to the aqueous phase containing 1% (w/v) PVA. The organic phase was then poured into the aqueous phase slowly and homogenized at 15,000 rpm for 7 min using a high-speed homogenizer (Heidolph, Germany). Subsequently, hot water (40 °C) was added to this oil/water emulsion under magnetic stirring (700 rpm) to evaporate the organic solvent overnight.

2.3. Preparation and characterization of chitosan/HAp scaffolds

Porous chitosan/HAp scaffolds were prepared by the freeze-drying method described in our previous study [21]. In brief, 2% (w/v) chitosan solution was prepared using distilled water containing 0.2 M acetic acid, and this solution was filtered through a 0.45 μm filter (Milipore, USA) to remove impurities. Then, differently from the previous study, 1.5% (w/v) HAp particles in bead form were added to the chitosan solution and mixed for 3 h using a magnetic stirrer. The solution was poured into 24-well tissue-culture polystyrene (TCPS) dishes and lyophilized for 3–4 days in a freeze-dryer (Christ, Germany). For neutralization, the scaffolds were left in a 1 M sodium carbonate solution for 2 h. Then they were washed with distilled water several times, until the pH of the washing solution was 7.0, and dried in freeze-dryer overnight.

2.3.1. SEM analysis

Dried scaffolds were coated with a thin layer of a palladium-gold alloy under vacuum and examined by Scanning Electron Microscope (SEM, Zeiss Evo 50, Germany). The average pore diameters were determined by using the ImageJ program (NIH, Bethesda, MD, USA).

2.3.2. Micro-computed tomography (μ-CT)

The scaffolds were scanned using micro-computed tomography (μ-CT; Bruker, Skyscan 1272) at 69 kV and 170 μA, with a 1 × ms exposure and 4 × magnification. The μ-CT analyzer software (CTAn, version 1.13, SkyScan, Bruker, Belgium) was used to calculate the porosity and closed pore percentages.

2.3.3. Mechanical analysis

The dried scaffolds were cut into cylindrical shapes of specific dimensions (9 mm diameter, 2 mm height) for mechanical testing using Texture Analyzer (TA.XT Plus, UK). These samples were swollen in phosphate-buffered saline (PBS, pH:7.4) at 37 °C for 1 h before testing.

2.3.4. Thermal gravimetric analysis

Thermogravimetric analysis (TGA) was carried out at 10 °C/min heating rate in the range of 25–600 °C in nitrogen atmosphere by using TG/DTA 6300 SII EXSTAR 6000 (Seiko Instruments Inc., USA).

2.4. Incorporation of melatonin-loaded PLGA microparticles into chitosan/HAp scaffolds

Melatonin-loaded PLGA microparticles were dispersed in a small amount of distilled water and homogenized at 6000 rpm for 30 s. They were then loaded into chitosan/HAp scaffolds by one of two different methods: (i) mixing into the chitosan solution during preparation of the scaffolds or (ii) embedding onto scaffolds after their preparation. In each case, 0.5 mg particles were loaded into each scaffold (9 mm in diameter, 2 mm in height) and the scaffolds were freeze-dried. Melatonin-carrying scaffolds were neutralized using the method described in Section 2.3. Three types of scaffolds (chitosan/HAp, chitosan/HAp + Mp, chitosan/HAp-Mp) were prepared and presented in Table 1.

2.5. In vitro melatonin release studies

In vitro melatonin release studies from chitosan/HAp scaffolds (9 mm × 2 mm) were carried out in 1.5 mL PBS (pH: 7.4) containing 0.1% (w/v) sodium azide at 37 °C and 70 rpm agitation for 40 days. The release studies were performed in dark due to the sensitivity of melatonin to light. At selected time points, 2 μL of supernatant was analyzed by NanoDrop 2000c Spectrophotometer (Thermo Scientific, USA) at 279 nm. The buffer solution was replenished after each measurement to obtain sink conditions.

2.6. Cell culture studies for osteogenic properties of scaffolds

2.6.1. Cell line maintenance and cell seeding onto scaffolds

To investigate the osteoinductive properties of the melatonin-carrying scaffolds, cell culture studies were carried out with the MC3T3-E1

Table 1
Chitosan-based scaffolds prepared in this study.

Name of sample	Description of sample
Chitosan/HAp	Control scaffold
Chitosan/HAp + Mp	Chitosan/HAp scaffolds loaded with melatonin-containing PLGA microparticles during manufacture
Chitosan/HAp−Mp	Chitosan/HAp scaffolds loaded with melatonin-containing PLGA microparticles via embedding
Chitosan/HAp + Mp(−)	Chitosan/HAp scaffolds loaded with blank PLGA microparticles during manufacture
Chitosan/HAp + Mp(−)/ic	Chitosan/HAp + Mp(−) scaffolds loaded with melatonin/HPβCD inclusion complex
Chitosan/HAp + Mp/ic	Chitosan/HAp + Mp scaffolds loaded with melatonin/HPβCD inclusion complex

Table 2
The primer sequences used in this study.

Genes		Primers
β-actin	Forward	5′-GTG CTA TGT TGC CCT AGA CTT CG-3′
	Reverse	5′-GAT GCC ACA GGA TTC CAT ACCC-3′
Col-1	Forward	5′-CAA GAT GTG CCA CTC TGA CT-3′
	Reverse	5′-TCT GAC CTG TCT CCA TGT TG-3′
RunX2	Forward	5′-GCA TGG CCA AGA AGA CAT CC-3′
	Reverse	5′-CCT CGG GTT TCC ACG TCTC-3′
Opn	Forward	5′-CAC TTT CAC TCC AAT CGT CCC TAC-3′
	Reverse	5′-ACT CCT TAG ACT CAC CGC TCT TC-3′
Ocn	Forward	5′-CTT TCT GCT CAC TCT GCTG-3′
	Reverse	5′-TAT TGC CCT CCT GCT TGG-3′

mouse osteoblastic cell line (Riken Cell Bank, Japan). The studies were conducted for 21 days with the three types of scaffolds given in Table 1, chitosan/HAp, chitosan/HAp + Mp, chitosan/HAp-Mp. Prior to the cell culture experiments, the scaffolds were sterilized in 70% (v/v) ethanol for 30 min and washed with Dulbecco's PBS (DPBS) three times. Both sides of the scaffolds were then exposed to UV light for 30 min. Following sterilization, scaffolds were placed in a proliferation medium (α-MEM medium containing 10%, v/v, FBS, 1%, v/v, penicillin–streptomycin) and were allowed to interact with serum proteins for 2 h. The cells were seeded onto the scaffolds in 30 μL of proliferation medium at 4×10^5 cells/mL. After 3 h, 1 mL proliferation medium was added to the scaffolds and the cell–scaffold constructs were incubated at 95% humidity and 5% CO_2. On the 5th day of culture, the proliferation medium was removed and replaced with 1 mL of osteogenic differentiation medium (10 mM β-glycerol phosphate and 50 μg/mL ascorbic-acid-added proliferation medium). During the culture period, the medium over the scaffolds was replenished by half every 2–3 days. All procedures requiring a sterile medium were performed in a laminar flow cabinet (Bioair, Type II Laminar Flow Cabinet, Italy).

2.6.2. Cell viability

Mitochondrial activities of preosteoblastic MC3T3-E1 cells on chitosan/HAp scaffolds were determined by MTT assay at various culture periods up to 21 days. At selected times, the culture medium was removed from the scaffolds and 600 μL pre-warmed culture medium supplemented with 60 μL MTT solution (2.5 mg/mL MTT dissolved in PBS) was added to each sample, which was then incubated at 37 °C for 3 h. Next, 400 μL of 0.04 M HCl containing isopropanol was added to each well to dissolve the purple formazan crystals. The optical density of 200 μL of the solution was measured spectrophotometrically at 570 nm with reference to 690 nm using a microplate reader (ASYS, Hitech UVM 340 plate reader, Austria).

2.6.3. Cellular morphology

The attachment, spreading, and morphology of the cells cultured on PLGA microparticle-loaded chitosan/HAp scaffolds were observed by SEM at the end of 7, 14, and 21 days of culture. After removal of the culture medium, the cell-seeded scaffolds were gently washed with PBS twice; the cells were then fixed with 2.5% (v/v) glutaraldehyde solution. After 30 min, the scaffolds were washed with PBS and kept at 4 °C. Then, they were dehydrated in ethanol series (30%, 50%, 70%, 90%, and 100%) for approx. 2 min at each concentration. The scaffolds were then dried in HMDS for 5 min and later dried in air after the removal of HMDS. When completely dry, the scaffolds were coated with a palladium–gold alloy and mounted on a SEM stub, before morphological observation by SEM.

2.6.4. ALP activity and collagen analysis

Early osteogenic differentiation of preosteoblastic MC3T3-E1 cells was determined by determination of ALP activity and collagen synthesis. On days 7, 14, and 21, the culture media over the scaffolds were removed and the scaffolds were washed twice with PBS (pH 7.4). Then ALP Assay Kit (BioVision, USA) was used in accordance with the manufacturer's protocol to determine the ALP activity. Collagen content was determined using Hydroxyproline Colorimetric Assay Kit (Biovision, USA) in accordance with the manufacturer's protocol.

2.6.5. Real time RT-PCR analysis

RT-PCR was carried out to determine the transcription levels of type 1 collagen (*Col-1*), runt-related transcription factor 2 (*RunX2*), osteopontin (*Opn*) and osteocalcin (*Ocn*). Expression levels of these genes were quantified using a LightCycler® Nano (Roche, Switzerland) and they were normalized to housekeeping gene *β*-actin. The data were calculated as fold change relative to control scaffolds (chitosan/HAp), according to the first day of analysis, using the $2^{-(\Delta\Delta Ct)}$ method. The primers for each gene are given in Table 2.

2.7. Preparation and characterization of melatonin/HPβCD inclusion complex-loaded scaffolds

The inclusion complex of melatonin and HPβCD was prepared by the microwave-induced method optimized in our previous study [22]. Briefly, stoichiometric amounts of HPβCD and melatonin were dissolved in 50% ethanol (v/v) and exposed to 900 W in a microwave oven (Milestone, Italy) at 60 °C for 90 s. The resulting solution was filtered through a 0.45 μm filter, to remove impurities, and dried under vacuum at 45 °C for three days. As a result, melatonin/HPβCD inclusion complex was obtained in the form of white powder. To load approx. 2 mg of melatonin into the chitosan/HAp scaffolds, 200 mg melatonin/HPβCD inclusion complex was dissolved in 2 mL distilled water. Then, six chitosan scaffolds (2 mm diameter, 9 mm height) were added to the solution and kept at 4 °C overnight. After being removed from the solution, the scaffolds were frozen at −20 °C for 4 h and then, lyophilized overnight.

2.7.1. SEM analysis

The incorporation of the melatonin/HPβCD inclusion complex into the chitosan/HAp scaffolds was observed by SEM, as explained in Section 2.3.

2.7.2. ATR–FTIR analysis

To examine whether the melatonin/HPβCD inclusion complex was successfully incorporated into the chitosan/HAp scaffolds, attenuated total reflectance Fourier transform infrared spectroscopy (ATR–FTIR) (Thermo Scientific Nicolet iS10, USA) analysis was performed at 500–4000 cm^{-1} wavelengths.

2.7.3. In vitro melatonin release studies

In vitro melatonin release studies from melatonin/HPβCD inclusion-complex-loaded chitosan/HAp scaffolds were carried out for 5 h in a shaker bath, which was maintained at 37 °C and shaken horizontally at 70 rpm in dark. The scaffold was placed in 5 mL and at selected times, 2 mL of release medium was analyzed by NanoDrop at 279 nm and the buffer solution was replenished after each measurement to provide the perfect sink conditions. The data were evaluated with the calibration curve explained in Section 2.5.

2.8. Cell culture studies for anticarcinogenic properties of scaffolds

MG-63 human osteosarcoma cells were subcultured in flasks using DMEM supplemented with 10% (v/v) FBS and 1% (v/v) antibiotic solution (penicillin–streptomycin) and incubated at 37 °C in a humidified CO_2 (5%) atmosphere. In this part, four different chitosan scaffolds given in Table 1 were used. These are:

chitosan/HAp + Mp(−), chitosan/HAp + Mp, chitosan/HAp + Mp(−)/ic and chitosan/HAp + Mp/ic.

Sterilization of the scaffolds was achieved by exposure to UV for 10 min. Before cell–scaffold interaction, MG-63 cells were trypsinized upon subconfluence, and 1×10^4 cells/cm^2 were seeded on 24-well plates. After 24 h, the sterile scaffolds were placed into the wells and 1 mL culture medium was added to each well. The cell culture was conducted in a 5% CO_2 atmosphere at 37 °C.

2.8.1. Cell viability

The effect of melatonin on the proliferation of MG-63 cells was determined using MTT assay for the 1st, 2nd, and 3rd days of culture. The same MTT procedure given in Section 2.6.2 was applied.

2.8.2. Cell cycle analysis

At the end of the 24 h cell–scaffold interaction, cell cycle analysis was performed. The scaffolds were removed, and the cells harvested by trypsinization were centrifugated at 1500 rpm for 5 min. Supernatant was then removed and the cells were washed with PBS and fixed in 70% (v/v) ice-cold ethanol and stored at −20 °C overnight. The cells were again rinsed with PBS and resuspended in 200 μL of PBS containing 10 μg/mL propidium iodide, 0.1% (v/v) Triton X-100, and 100 μg/mL DNase-free RNase. Each sample was kept in the dark at room temperature for 30 min. Two thousand events were acquired with a BD FACS Calibur Flow Cytometer (USA) for each sample, and the percentage of cells in G_0/G_1, S, and G_2/M phases of the cell cycle were determined by Modfit LT 3.0 analytical software.

2.9. Statistical analysis

The experiments were carried out in triplicate, and all data were expressed as mean ± standard deviation. Statistical analysis was performed by GraphPad InStat software (GraphPad, USA). One-way ANOVA was used to determine significant differences among the groups and $*p < 0.05$, $**p < 0.01$, and $***p < 0.001$ represent statistically significant, very significant, and extremely significant values, respectively; whereas $p > 0.05$ represents no statistically significant values.

3. Results

3.1. Characterization of chitosan/HAp scaffolds

The pore sizes of the chitosan/HAp scaffolds were ~190 μm with interconnected morphology, and HAp particles were present in the structure (Fig. 1a). For detailed morphological examination, μ-CT analysis was performed. In the three-axis general view of the scaffold, it was determined that the scaffold has a highly porous structure (Fig. 1b). Porosity and closed pore percentages were calculated from μ-CT data. These values and some other basic properties of the chitosan/HAp scaffolds are given in Table 3.

3.2. Incorporation of melatonin-loaded PLGA microparticles into chitosan/HAp scaffolds

Preparation conditions and some properties of both blank and melatonin-loaded PLGA microparticles are summarized in Table 3. PLGA microparticles were homogeneously distributed into the scaffolds and did not change the interconnected morphology of the scaffolds. However, the particles were quite integrated with the scaffold when they were loaded into the structures during production (Fig. 1 **c, d**). Further, the microparticles were distributed much more separately in the chitosan/HAp scaffold when the particles were loaded by the post-production embedding method (Fig. 1 **e, f**).

3.3. In vitro melatonin release studies

The *in vitro* release of melatonin from chitosan/HAp scaffolds containing PLGA microparticles was performed for 40 days. For the quantification of released melatonin amounts, calibration curve was used. The calibration curve was assessed in PBS and was linear in the range of standard concentration at 0–250 μg/mL with a regression equation: $y = 0.003x + 0.0039$ (y, absorbance; x, concentration of melatonin in PBS, mg/mL), $r^2 = 0.9999$. The range of melatonin concentration for the determination of calibration curve was selected by taking into consideration of melatonin solubility in release conditions. There are some different opinions about the solubility of melatonin in literature. Most discussions of melatonin have assumed that this molecule is highly hydrophobic. Contrary to belief, melatonin is thought to be an amphiphilic molecule [23,24] and has higher solubility in water. Shida et al. [25], determined that, melatonin is soluble in aqueous medium up to 5×10^{-3} M which leads to ~1.16 g/L. Hamed et al. [26] stated the aqueous solubility of melatonin is 0.96 g/L at 25 °C. In addition, the solubility of melatonin was examined in our experiments and it was dissolved up to 1 g/mL concentration in water and PBS. Therefore, the concentrations in calibration curve are in the range of melatonin solubility.

Cumulative melatonin release curves are given in Fig. 2a. Approximately 45% and 70% of melatonin were released with burst effect from chitosan/HAp + Mp and chitosan/HAp − Mp scaffolds, respectively, in 24 h. At the end of the 40-day release, ~62% and ~98% of the loaded melatonin were released by a controlled and slow diffusion mechanism from chitosan/HAp + Mp and chitosan/HAp − Mp scaffolds, respectively. The results of i*n vitro* release studies are also summarized in Fig. 2b. These released amounts correspond to ~40 μM and ~70 μM concentrations in the cell culture media for chitosan/HAp + Mp and chitosan/HAp − Mp scaffolds, respectively.

3.4. Osteogenic properties of melatonin-releasing scaffolds

The results of MTT analysis of MC3T3-E1 cells within the scaffolds are given in Fig. 3a. Especially on days 7 and 14, the mitochondrial activities of the cells cultured on PLGA microparticle-loaded scaffolds (chitosan/HAp + Mp and chitosan/HAp − Mp) were statistically higher than that of a chitosan/HAp control group ($p < 0.05$).

The ALP activities of the cells cultured on chitosan/HAp + Mp and chitosan/HAp − Mp scaffolds on days 7 and 14 were significantly higher (~2 fold) than that of control group, chitosan/HAp scaffolds ($p < 0.001$) (Fig. 3b). On the 7th day of culture, the amount of collagen synthesized by cells proliferating in chitosan/HAp + Mp and chitosan/HAp − Mp scaffolds was significantly higher (~2.3 fold) than that of the control group ($p < 0.01$). On the 14th day of culture, again there was a statistical difference between the hydroxyproline amounts of the microparticle-loaded scaffolds and of the control ($p < 0.05$). On day 21, no significant difference was observed among groups ($p > 0.05$) for both ALP activity and collagen synthesis (Fig. 3b and c).

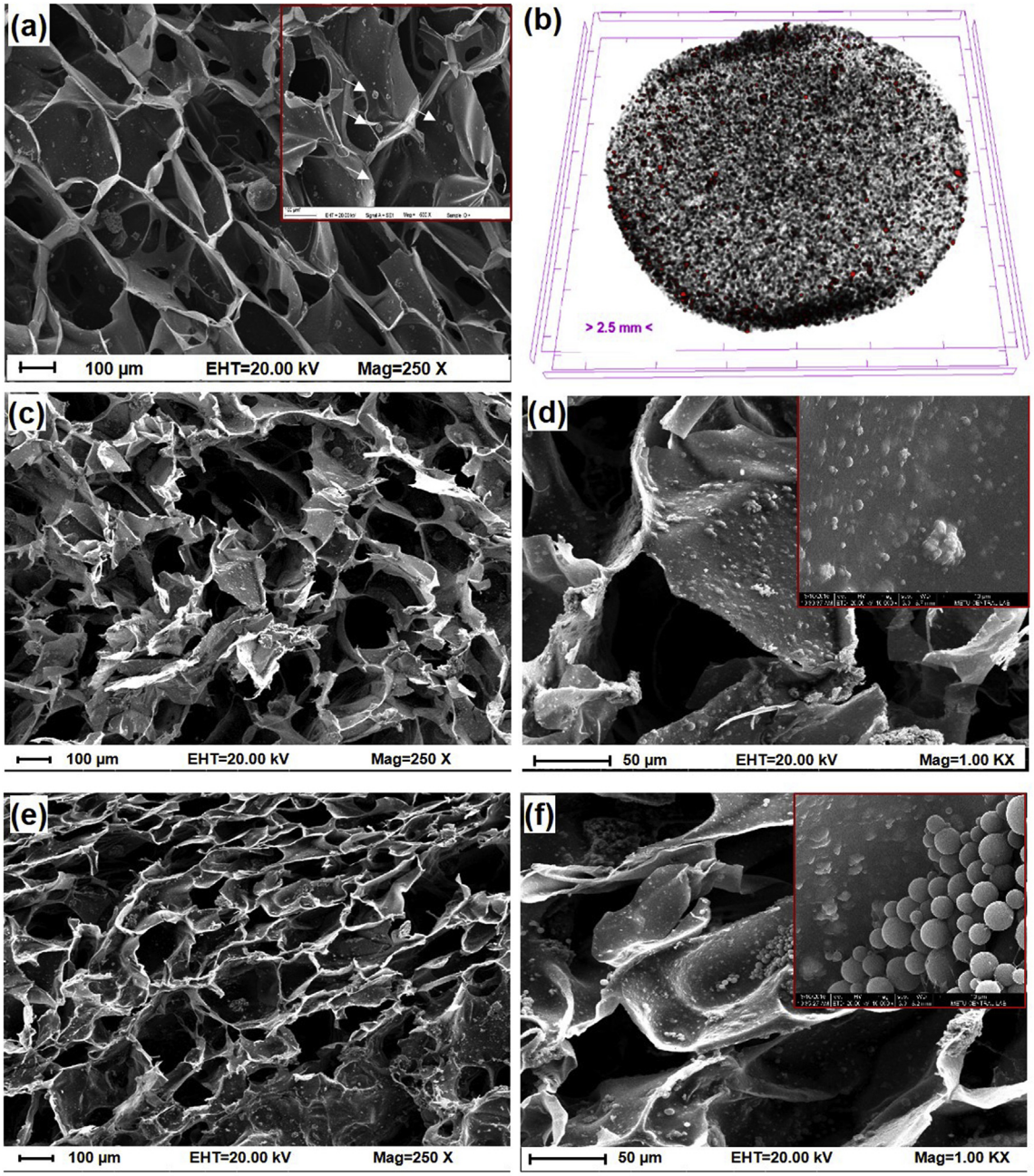

Fig. 1. (a) SEM image of chitosan/HAp scaffold (HAp particles are indicated by white arrows); (b) µ-CT image of chitosan/HAp scaffold at the xyz axis; SEM images of PLGA microparticle loaded chitosan/HAp scaffolds at different magnifications; (c) chitosan/HAp + Mp (250 ×); (d) chitosan/HAp + Mp (1000 ×); (e) chitosan/HAp − Mp (250 ×); (f) chitosan/HAp − Mp (1000 ×). Higher magnifications are given on the top right-hand corner (10,000 ×).

Table 3
Some basic properties of chitosan/HAp scaffolds and PLGA microparticles.

Chitosan/HAp Scaffolds	Average pore diameter (µm)	Onset of T_D[a] (°C)	Elastic modulus (N/mm^2)	Total porosity (%)	Closed pores (%)
	196.31 ± 63.50	230	2.2 ± 0.7	62.9	0.14
PLGA particles	Homogenization conditions	Average size (µm)	Encapsulation efficiency (%)	Loaded amounts (µg melatonin/mg particle)	
Blank	15,000 rpm 7 min	3.18 ± 1.03	–	–	
Melatonin-loaded	15,000 rpm 7 min	3.67 ± 1.64	17.3 ± 3.4	34.0 ± 4.3	

[a] T_D: thermal degradation temperature.

In addition, ALP and collagen levels increased from day 7–21 for control group ($p < 0.01$). While controlled release of melatonin from chitosan/HAp + Mp and chitosan/HAp-Mp scaffolds was inducing osteogenic differentiation of cells with increased ALP activity and collagen in the early days of culture, these markers increased by time up to 21 day in control group.

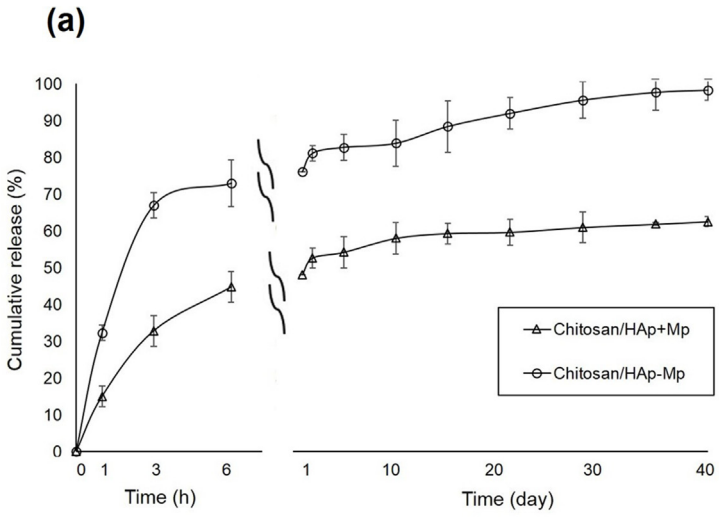

(b)

Released amounts (μg melatonin/scaffold)						
Scaffolds	**1 h**	**1 day**	**5 day**	**10 day**	**20 day**	**40 day**
Chitosan/HAp+Mp	2.55 ± 0.48	8.11 ± 0.47	9.64 ± 0.01	9.83 ± 0.01	10.06 ± 0.18	10.55 ± 0.45
Chitosan/HAp-Mp	5.49 ± 0.36	12.83 ± 1.19	13.96 ± 0.84	14.14 ± 0.84	15.53 ± 0.13	16.60 ± 0.13

Fig. 2. *In vitro* release profiles of melatonin from chitosan/HAp scaffolds: (a) cumulative release kinetics; (b) cumulative amounts of melatonin released from chitosan/HAp scaffolds.

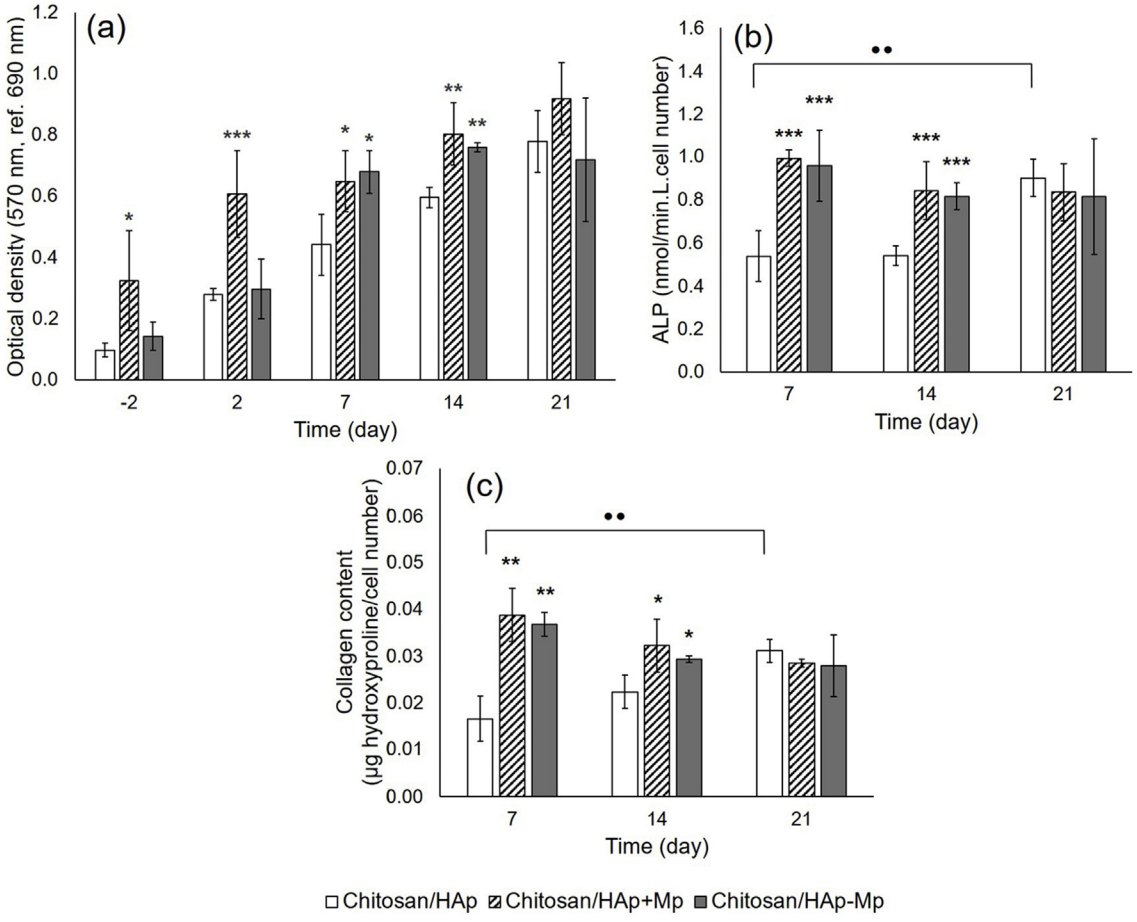

Fig. 3. The results of the cellular behaviors of MC3T3-E1 cells cultured on chitosan/HAp-based scaffolds: (a) mitochondrial activities of the cells; (b) ALP activities of the cells; (c) collagen content of the cells. (Statistically significant differences, n = 3: $*p < 0.05$, $**p < 0.01$, $***p < 0.001$ when chitosan/HAp is a control group; $\bullet\bullet p < 0.01$ when chitosan/HAp at day 7 is a control group).

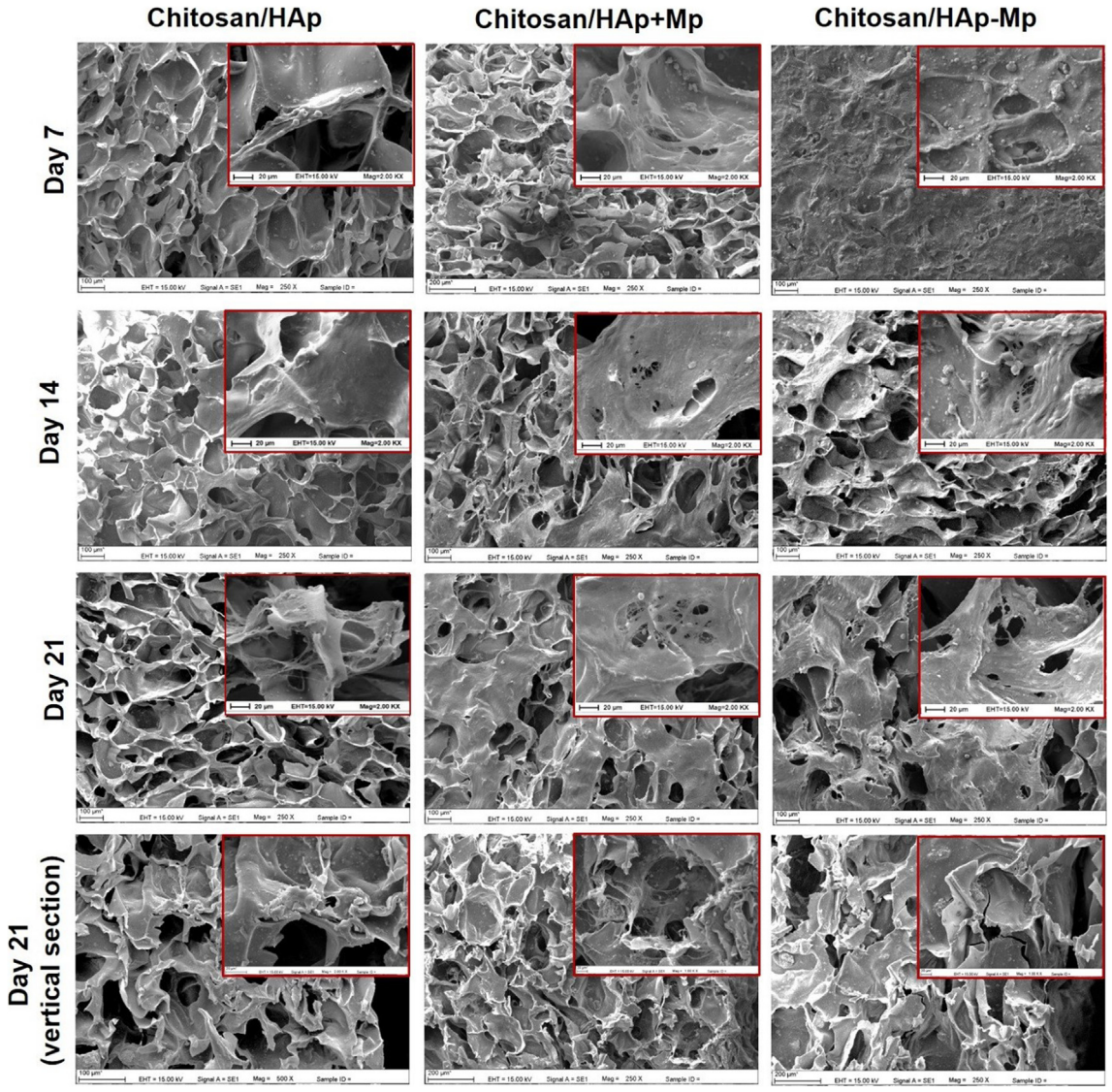

Fig. 4. SEM images of MC3T3-E1 cells cultured on the chitosan/HAp-based scaffolds at days 7, 14, and 21 (250 ×). Higher magnifications are given in the top right-hand corners (2000 ×).

SEM images of the scaffolds at the 7th, 14th, and 21st days of culture are given in Fig. 4. The cells were successfully attached and proliferated on all types of the scaffolds at day 7. However, more cells were observed in chitosan/HAp + Mp and chitosan/HAp − Mp scaffolds. The vertical sections of these scaffolds taken on the 21st day of culture showed that the cells migrated inside the pores of the scaffolds and the cells found at depths of approximately 600–700 μm from the scaffold surface. The cells almost covered the entire scaffold and mineral clusters showing bone differentiation were observed in the scaffolds containing PLGA microparticles.

Fig. 5a and b showed that the *Col-1* and *RunX2* expression levels of cells in the chitosan/HAp + Mp ($p < 0.001$) and chitosan/HAp − Mp ($p < 0.01$) groups were higher than that of the chitosan/HAp group on the 14th day of culture. On the 14th day of culture, *Opn* expression levels of cells cultured in chitosan/HAp + Mp and chitosan/HAp − Mp scaffolds were significantly higher than that of the control ($p < 0.01$) (Fig. 5c). The *Ocn* expression levels of chitosan/HAp + Mp ($p < 0.001$) and chitosan/HAp − Mp ($p < 0.01$) groups on day 21 were significantly higher than that of the control (Fig. 5d).

3.5. Characterization of melatonin/HPβCD inclusion-complex-loaded scaffolds and in vitro cell culture studies

The SEM photographs show that the melatonin/HPβCD inclusion complex was homogeneously distributed in the chitosan/HAp scaffolds and the scaffold porosity was not affected negatively (Fig. 6a). In addition, the irregular particles expressing amorphous structure prove the formation of melatonin/HPβCD inclusion complex. Unlike the peaks in the FTIR spectrum of chitosan/HAp, the broad peak seen at the wavelength of 3350 cm^{-1} belongs to the OH groups in HPβCD. The peaks at 945 and 855 cm^{-1} belong to the asymmetric tensile vibrations of methylene groups in HPβCD in the spectrum of chitosan/HAp/ic in Fig. 6b [27,28]. The presence of all these peaks belong to HPβCD proves that the melatonin/HPβCD inclusion complex is successfully incorporated into the scaffold structure.

In vitro melatonin release kinetics from melatonin/HPβCD-loaded chitosan/HAp scaffolds are presented in Fig. 6c. Approximately 80% (~2.02 mg) of melatonin was rapidly released within 20 min, and the remaining melatonin was released over 5 h (~2.27 mg). This immediate and short-term melatonin release is required to inhibit proliferation of MG-63 cells.

Fig. 6d showed that the optical density of the chitosan/HAp + Mp

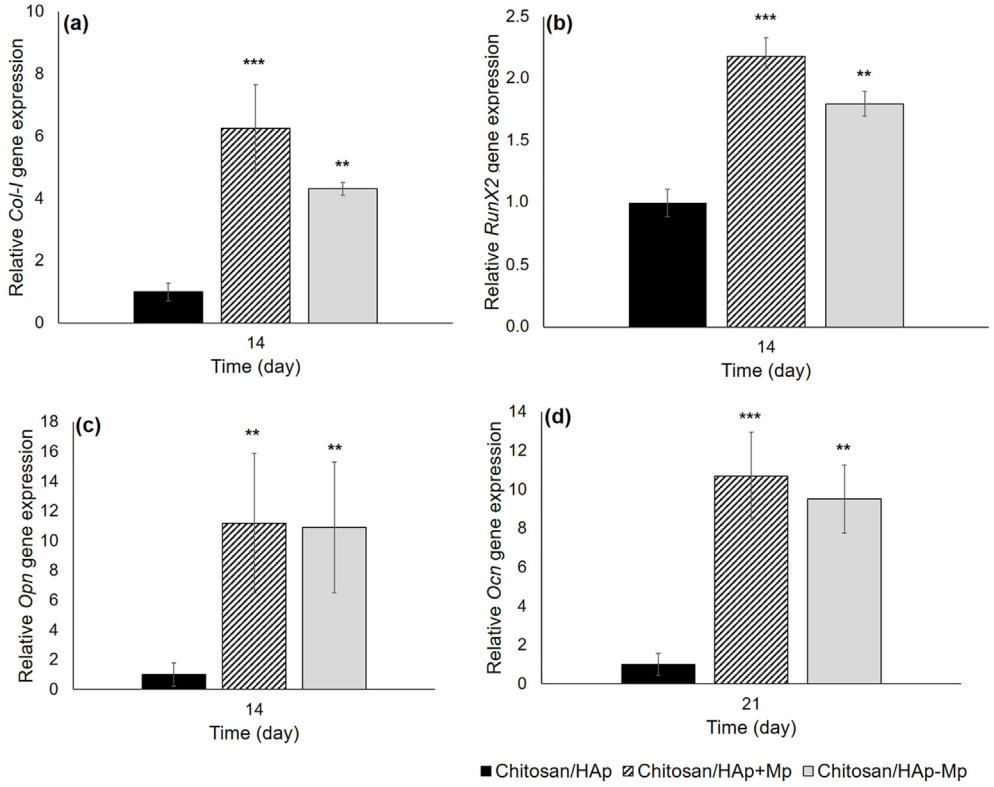

Fig. 5. Gene expression levels of: (a) *Col-1*; (b) *RunX2*; (c) *Opn*; (d) *Ocn* for MC3T3-E1 cells cultured on chitosan/HAp-based scaffolds. (Statistically significant differences: n = 3, $*p < 0.05$, $**p < 0.01$, $***p < 0.001$ when chitosan/HAp is the control group).

(−)/ic group was significantly lower than that of the control on the first day of culture ($p < 0.001$). Melatonin released from both inclusion-complex-loaded scaffolds i.e. chitosan/HAp + Mp(−) and chitosan/HAp + Mp/ic significantly decreased the proliferation of the cells on the 2nd and 3rd days of culture ($p < 0.001$).

To determine whether melatonin caused a change in cell cycle distribution, cell cycle analysis was performed using flow cytometry at the 1st day of cell–scaffold interaction and the results are given in Fig. 6e. The cell fractions in the G_0/G_1 phase for both melatonin/HPβCD inclusion-complex-loaded chitosan scaffolds increased significantly compared with those of the control ($p < 0.01$). No difference observed in the S phase among the groups ($p > 0.05$). In addition, the cell numbers in the G_2/M phase for inclusion-complex-containing groups were significantly lower than those of the control ($p < 0.01$). As a result, it was determined that melatonin released from the inclusion-complex-loaded chitosan/HAp scaffolds inhibited the proliferation of MG-63 human osteosarcoma cells in the G_0/G_1 phase.

4. Discussion

Although melatonin carrying particular systems has recently been developed and investigated for bone regeneration [2,20,23,29], melatonin loaded 3D scaffolds has so far not been developed. Here, we prepared a melatonin-releasing 3D scaffold-based device to be locally implanted into the damaged area after surgical removal of tumor in order to promote bone regeneration and inhibit cancer cells left in the surrounding tissue. This is why, chitosan scaffolds were supported by osteoinductive component, HAp beads, and melatonin releasing systems, PLGA microparticles and melatonin/HPβCD inclusion complex. Experimental observations showed that HAp beads were successfully distributed within the chitosan scaffolds in suitable pore sizes. It is known that while large pores (100–200 μm) are necessary for substantial bone growth, smaller pores cause ingrowth of both fibrous and unmineralized osteoid tissue [30]. The scaffold is also thermally stable after neutralization with sodium carbonate. The compression modulus of chitosan/HAp scaffolds was determined as ~2.2 N/mm^2, and when this value is compared with the ultimate compressive strength of trabecular bone (0.22–10.44 N/mm^2), it is acceptable [31] Another case, it is thought that there is a surface interaction by which the particles remain attached to the scaffold surface when they were loaded by the postproduction embedding method. There is an electrostatic attraction between PLGA microparticles and chitosan because of the negatively charged carboxyl groups in PLGA and positively charged amino groups in chitosan. In addition, there may be an interaction between negatively charged PLGA and hydroxyapatite due to the positive calcium ions and negative phosphate ions in HAp.

Low encapsulation efficiency was obtained for PLGA microparticles due to the amphiphilic structure of melatonin and this situation is in accordance in literature as explained in our previous study [20]. In order to achieve the controlled and sustained release of melatonin, 0.5 mg of PLGA microparticles carrying ~17 μg melatonin were incorporated into each chitosan/HAp scaffold (~7 mg). The *in vitro* melatonin release studies showed that scaffolds exhibited a biphasic melatonin release-profile, which was an initial burst effect within 24 h followed by a sustained release over 40 days by Fickian diffusion. High burst effect may be explained by the plasticizing effect of melatonin on PLGA microparticles. Pandey et al. [32], stated that, 10% (w/w) melatonin loaded poly(D,L-lactic acid) (PLA) nanoparticles has lower glass transition temperature (T_g: 67 °C) than that of blank PLA nanoparticles (T_g: 70 °C). In our study, T_g values of blank and melatonin loaded PLGA microparticles were determined as 46.5 °C and 45.0 °C, respectively (data not shown). Approximately 3% of melatonin was incorporated into the PLGA microparticles and 1.5 °C decrease in T_g value may have thought to be due to the plasticizing effect of encapsulated melatonin. In addition, the burst release may have caused due to the contribution of water that can depress the T_g up to 15 °C bringing the polymer to a rubbery state at the release temperature [33]. Also, the diffusion coefficient of small molecules (e.g., melatonin) through the polymer

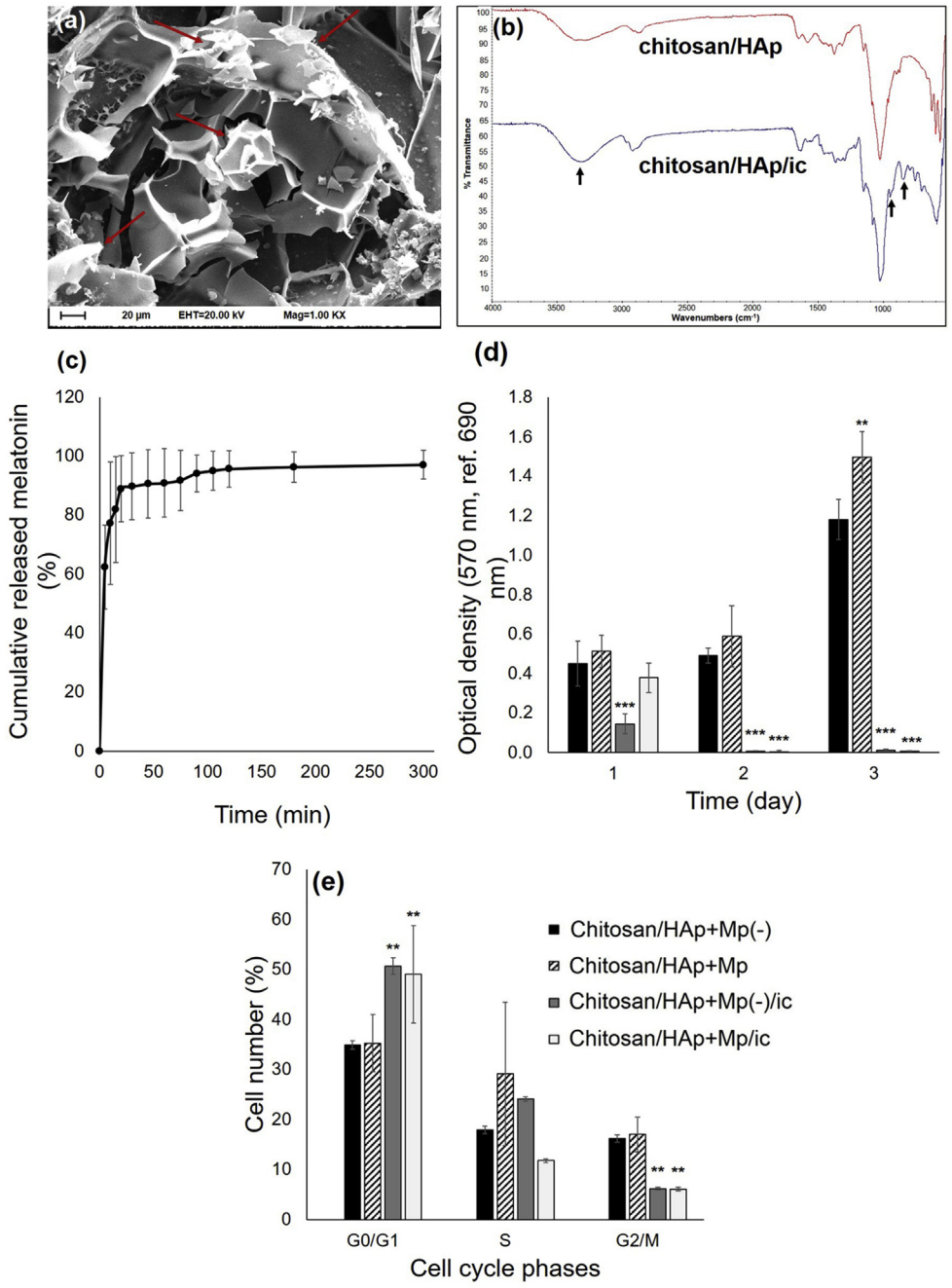

Fig. 6. (a) SEM image of melatonin/HPβCD inclusion-complex-loaded chitosan/HAp scaffold; (b) ATR–FTIR spectra of chitosan/HAp and chitosan/HAp/ic; (c) cumulative released melatonin percentage; (d) effect of melatonin on viability of MG-63 cells; (e) cell cycle distribution in MG-63 cells. (Statistically significant differences: n = 3, $*p < 0.05$, $**p < 0.01$, $***p < 0.001$ when chitosan/HAp + Mp(−) is the control group).

matrix may increase by several orders of magnitude upon transition from the glassy to the rubbery state [34].

Due to the increase of the diffusion pathway, melatonin released more slowly from the scaffolds that were prepared by incorporating the PLGA microparticles during production when compared with the melatonin release from the scaffolds prepared by embedding the microparticles after production. In addition, the microparticles were incorporated into the chitosan structure better and slightly agglomerated in chitosan/HAp + Mp when compared to chitosan/HAp-Mp. Therefore, faster release was obtained for the scaffolds prepared by embedding the microparticles after production. The *in vitro* release studies showed that melatonin concentrations that will be released to the cell culture medium from PLGA microparticle-loaded chitosan/HAp scaffolds is in the micromolar range (~40–70 µM). Several studies have emphasized that micromolar concentrations of melatonin promote the proliferation of bone cells [1,3,5,35,36]. According to the MTT results in our study, the positive effect of melatonin on cell viability and proliferation was observed in microparticle-loaded scaffolds, especially within 14 days.

ALP is an essential enzyme in bone matrix mineralization and its activity is high before the start of calcium deposition [37]. Recent studies showed that ALP activity and/or collagen type I synthesis of preosteoblasts/osteoblasts increases dose-dependently in the presence of free melatonin from nanomolar to 250 µM concentration [1,3,5,38]. It is also reported that long-term sustained release of melatonin from PLGA microparticles interacted with hMSCs also improved ALP activity

[2]. The results in our study suggest that, controlled release of melatonin from chitosan/HAp + Mp and chitosan/HAp − Mp scaffolds promoted ALP activity at days 7 and 14 compared to control group and then ALP levels decreased or remained constant at day 21. This may be caused because the controlled release of melatonin promoted osteogenic differentiation of MC3T3-E1 cells in the early periods of culture and the expression of this enzyme is downregulated after mineralization starts. In addition, control group has the highest ALP activity at day 21, which shows that the cells differentiated to osteoblasts later than the other melatonin containing scaffolds. The primary function of differentiated osteoblasts is collagen synthesis. So collagen is a specific gene of early- and mid-stage of osteogenesis. Similar results were obtained for collagen synthesis as in the ALP activity and it can be concluded that, sustained release of melatonin from these scaffolds promoted early osteogenic differentiation of preosteoblastic MC3T3-E1 cells.

Melatonin promotes gene expression of some bone markers such as ALP, *Ocn*, *RunX2*, *Opn*, *Col-I*, and bone sialoprotein for several cell types, including MC3T3-E1 preosteoblasts and mesenchymal stem cells [1,2,4,38]. During the formation of new bone, cell proliferation first occurs, and osteoblasts secrete *Col-1*. In our study, the cells cultured within microparticle-loaded scaffolds showed higher expression levels of *Col-1* at day 14 than that of the control. *RunX2*, a major transcription factor in early osteoblast differentiation, triggers the expression of important bone matrix proteins. The cells proliferating within the microparticle-loaded scaffolds showed the highest *RunX2* gene expression at day 14.

Opn is a phosphorylated glycoprotein and is secreted by immature osteoblasts in the early periods of culture [39]. Chitosan/HAp + Mp and chitosan/HAp − Mp scaffolds exhibited the highest *Opn* expressions at day 14. *Ocn* is a marker of mature osteoblast formation and is synthesized in the late stages of differentiation. In a recent study by Son et al. [5], melatonin concentrations in the range of 50–250 μM significantly increased *Ocn* expressions of MC3T3-E1 cells under hypoxic conditions. Zhang et al. [2] also demonstrated that the micromolar concentrations of melatonin released from PLGA microparticles increased *Ocn* expressions of hMSCs. The high levels of *Ocn* gene expressions obtained for chitosan/HAp + Mp and chitosan/HAp − Mp scaffolds at day 21 indicated that these scaffolds are suitable for the differentiation of preosteoblastic MC3T3-E1 cells, and the results are in accordance with the literature.

It has been shown that melatonin has an oncostatic effect on various cancers and that milimolar concentrations on osteosarcoma cells have been shown to reduce cell proliferation [11]. However, the solubility of melatonin in water is low (~2 g/L), and its use is limited due to this [19]. On the other hand, the amphiphilic structure possessed by the melatonin is also well suited for inclusion-complex formation by its entering the hydrophobic cavity of the cyclodextrins [19,22]. Therefore, we decided to prepare melatonin/HPβCD inclusion complex to inhibit osteosarcoma cells by loading high amounts of melatonin into the scaffolds and by rapid melatonin release. The SEM photographs and the ATR–FTIR spectrum proved that the inclusion complex was successfully loaded into the scaffold. Melatonin rapidly released from the scaffolds within 5 h and the released melatonin concentration was approximately 8 mM, which is a desired concentration for the inhibition of MG-63 cells. The results of cell cycle analysis showed that this concentration of increased the number of cells in the G_0/G_1 phase while decreasing the number of cells in the G_2/M phase. These results are consistent with the literature [11].

5. Conclusion

In the present study 3D scaffold-based system in which both the osteoinductive and anticarcinogenic properties of melatonin can be effective together was developed. For patients with osteosarcoma, implantation of this system to the damaged area after surgery is thought to remove the remaining cancer cells in the surrounding tissue and promote the formation of new bone tissue, by temporarily supporting the damaged region. Our results concluded that, melatonin-releasing chitosan/HAp scaffold supported with high and low amount melatonin releasing systems, melatonin/HPβCD inclusion complex and PLGA microparticles, respectively, is a promising system for human osteosarcoma treatment and can be an adjunct to the routine chemotherapy of osteosarcoma.

Conflicts of interest

The authors have declared that there is no conflict of interest.

Author contributions

D. Çetin Altındal and M. Gümüşderelioğlu conceived the initial idea and the conceptualization; D. Çetin Altındal designed and performed the experiments, collected and analyzed the data. D. Çetin Altındal wrote the manuscript. M. Gümüşderelioğlu revised the manuscript. All authors have read and approved the final manuscript.

Acknowledgement

This study was supported by Hacettepe University Research Fund Project No. FBA-2015–5315.

Appendix A. Supplementary data

Supplementary data to this article can be found online at https://doi.org/10.1016/j.jddst.2019.05.027.

References

[1] K. Satomura, S. Tobiume, R. Tokuyama, Y. Yamasaki, K. Kudoh, E. Maeda, M. Nagayama, Melatonin at pharmacological doses enhances human osteoblastic differentiation in vitro and promotes mouse cortical bone formation in vivo, J. Pineal Res. 42 (3) (2007) 231–239 https://doi.org/10.1111/j.1600-079X.2006.00410.x.

[2] L. Zhang, J. Zhang, Y. Ling, C. Chen, A. Liang, Y. Peng, H. Chang, P. Su, D. Huang, Sustained release of melatonin from poly (lactic-co-glycolic acid) (PLGA) microspheres to induce osteogenesis of human mesenchymal stem cells in vitro, J. Pineal Res. 54 (1) (2013) 24–32 https://doi.org/10.1111/j.1600-079X.2012.01016.x.

[3] O. Nakade, H. Koyama, H. Ariji, A. Yajima, T. Kaku, Melatonin stimulates proliferation and type I collagen synthesis in human bone cells in vitro, J. Pineal Res. 27 (2) (1999) 106–110 https://doi.org/10.1111/j.1600-079X.1999.tb00603.x.

[4] N.M. Radio, J.S. Doctor, P.A. Witt-Enderby, Melatonin enhances alkaline phosphatase activity in differentiating human adult mesenchymal stem cells grown in osteogenic medium via MT2 melatonin receptors and the MEK/ERK (1/2) signaling cascade, J. Pineal Res. 40 (4) (2006) 332–342 https://doi.org/10.1111/j.1600-079X.2006.00318.x.

[5] J.H. Son, Y.C. Cho, I.Y. Sung, I.R. Kim, B.S. Park, Y.D. Kim, Melatonin promotes osteoblast differentiation and mineralization of MC3T3-E1 cells under hypoxic conditions through activation of PKD/p38 pathways, J. Pineal Res. 57 (4) (2014) 385–392 https://doi.org/10.1111/jpi.12177.

[6] M. Takechi, S. Tatehara, K. Satomura, K. Fujisawa, M. Nagayama, Effect of FGF-2 and melatonin on implant bone healing: a histomorphometric study, J. Mater. Sci. Mater. Med. 19 (8) (2008) 2949–2952 https://doi.org/10.1007/s10856-008-3416-3.

[7] S. Sethi, N.M. Radio, M.P. Kotlarczyk, C.T. Chen, Y.H. Wei, R. Jockers, P.A. Witt-Enderby, Determination of the minimal melatonin exposure required to induce osteoblast differentiation from human mesenchymal stem cells and these effects on downstream signaling pathways, J. Pineal Res. 49 (3) (2010) 222–238 https://doi.org/10.1111/j.1600-079X.2010.00784.x.

[8] C.R. Hoffmeister, T.L. Durli, S.R. Schaffazick, R.P. Raffin, E.A. Bender, R.C. Beck, A.R. Pohlmann, S.S. Guterres, Hydrogels containing redispersible spray-dried melatonin-loaded nanocapsules: a formulation for transdermal-controlled delivery, Nanoscale Res. Lett. 7 (1) (2012) 251–264 https://doi.org/10.1186/1556-276X-7-251.

[9] A. Cutando, J. Aneiros-Fernandez, J. Aneiros-Cachaza, S. Arias-Santiago, Melatonin and cancer: current knowledge and its application to oral cavity tumours, J. Oral Pathol. Med. 40 (8) (2011) 593–597 https://doi.org/10.1111/j.1600-0714.2010.01002.x.

[10] Y. Cheng, L. Cai, P. Jiang, J. Wang, C. Gao, H. Feng, C. Wang, H. Pan, Y. Yang, SIRT1 inhibition by melatonin exerts antitumor activity in human osteosarcoma cells, Eur. J. Pharmacol. 715 (1–3) (2013) 219–229 https://doi.org/10.1016/j.ejphar.2013.05.017.

[11] L. Liu, Y. Xu, R.J. Reiter, Melatonin inhibits the proliferation of human

osteosarcoma cell line MG-63, Bone 55 (2) (2013) 432–438 https://doi.org/10.1016/j.bone.2013.02.021.
[12] P. Lissoni, S. Barni, A. Ardizzoia, G. Tancini, A. Conti, G. Maestroni, A randomized study with the pineal hormone melatonin versus supportive care alone in patients with brain metastases due to solid neoplasms, Cancer 73 (3) (1994) 699–701.
[13] R.J. Reiter, S.A. Rosales-Corral, D.-X. Tan, D. Acuna-Castroviejo, L. Qin, S.-F. Yang, K. Xu, Melatonin, a full service anti-cancer agent: inhibition of initiation, progression and metastasis, Int. J. Mol. Sci. 18 (4) (2017) 843–890 https://doi.org/10.3390/ijms18040843.
[14] M.M. Leon-Blanco, J.M. Guerrero, R.J. Reiter, J.R. Calvo, D. Pozo, Melatonin inhibits telomerase activity in the MCF-7 tumor cell line both in vivo and in vitro, J. Pineal Res. 35 (3) (2003) 204–211 https://doi.org/10.1034/j.1600-079X.2003.00077.x.
[15] A. Panzer, Melatonin in osteosarcoma: an effective drug? Med. Hypotheses 48 (6) (1997) 523–525.
[16] A.M. Khattabi, W.H. Talib, D.A. Alqdeimat, A targeted drug delivery system of anticancer agents based on folic acid-cyclodextrin-long polymer functionalized silica nanoparticles, J. Drug Deliv. Sci. Technol. 41 (2017) 367–374 https://doi.org/10.1016/j.jddst.2017.07.025.
[17] W. Misiuk, M. Zalewska, Investigation of inclusion complex of trazodone hydrochloride with hydroxypropyl-β-cyclodextrin, Carbohydr. Polym. 77 (3) (2009) 482–488 https://doi.org/10.1016/j.carbpol.2009.01.033.
[18] E.M.M. Del Valle, Cyclodextrins and their uses: a review, Process Biochem. 39 (9) (2004) 1033–1046 https://doi.org/10.1016/S0032-9592(03)00258-9.
[19] D. Bongiorno, L. Ceraulo, A. Mele, W. Panzeri, A. Selva, V. Turco Liveri, Structural and physicochemical characterization of the inclusion complexes of cyclomaltooligosaccharides (cyclodextrins) with melatonin, Carbohydr. Res. 337 (8) (2002) 743–754 https://doi.org/10.1016/S0008-6215(02)00049-6.
[20] D. Çetin Altindal, M. Gumusderelioglu, Melatonin releasing PLGA micro/nanoparticles and their effect on osteosarcoma cells, J. Microencapsul. 33 (1) (2016) 53–63 https://doi.org/10.3109/02652048.2015.1115901.
[21] R.S. Tigli, A. Karakecili, M. Gumusderelioglu, In vitro characterization of chitosan scaffolds: influence of composition and deacetylation degree, J. Mater. Sci. Mater. Med. 18 (9) (2007) 1665–1674 https://doi.org/10.1007/s10856-007-3066-x.
[22] B. Topal, D. Cetin Altindal, M. Gumusderelioglu, Melatonin/HPbetaCD complex: microwave synthesis, integration with chitosan scaffolds and inhibitory effects on MG-63 Cells, Int. J. Pharm. 496 (2) (2015) 801–811 https://doi.org/10.1016/j.ijpharm.2015.11.028.
[23] T. Musumeci, C. Bucolo, C. Carbone, R. Pignatello, F. Drago, G. Puglisi, Polymeric nanoparticles augment the ocular hypotensive effect of melatonin in rabbits, Int. J. Pharm. 440 (2) (2013) 135–140 https://doi.org/10.1016/j.ijpharm.2012.10.014.
[24] J. Liu, F. Huang, H.-W. He, Melatonin effects on hard tissues: bone and tooth, Int. J. Mol. Sci. 14 (2013) 10063–10074 https://doi.org/10.3390/ijms140510063.
[25] C.S. Shida, A.M.L. Castrucci, M.T. Lamy-Freund, High melatonin solubility in aqueous medium, J. Pineal Res. 16 (1994) 198–201 https://doi.org/10.1111/j.1600-079X.1994.tb00102.x.
[26] M.Y. Hamed, E.M. Mostafa, S.S. Tous, Antifertility effect of orally formulated melatonin tablets in mice, Int. J. Pharm. 69 (1991) 93–102 https://doi.org/10.1016/0378-5173(91)90214-9.
[27] A. Corciova, B. Cioroiu, C. Mircea, C. Tuchilus, C. Ciobanu, C. Dimitriu, B. Ivanesvu, Influence of hydroxypropyl-beta-cyclodextrin on the physicochemical and biological characteristics of a flavone with important pharmacological properties, Environ. Eng. Manag. J. 14 (2) (2015) 311–319 https://doi.org/10.30638/eemj.2015.031.
[28] S.J. George, D.T. Vasudevan, Studies on the preparation, characterization, and solubility of 2-HP-β-cyclodextrin-meclizine HCl inclusion complexes, J. Young Pharm. 4 (4) (2012) 220–227 https://doi.org/10.4103/0975-1483.104365.
[29] A. Hafner, J. Lovric, D. Voinovich, J. Filipovic-Grcic, Melatonin-loaded lecithin/chitosan nanoparticles: physicochemical characterisation and permeability through Caco-2 cell monolayers, Int. J. Pharm. 381 (2) (2009) 205–213 https://doi.org/10.1016/j.ijpharm.2009.07.001.
[30] V. Karageorgiou, D. Kaplan, Porosity of 3D biomaterial scaffolds and osteogenesis, Biomaterials 26 (27) (2005) 5474–5491 https://doi.org/10.1016/j.biomaterials.2005.02.002.
[31] C.E. Misch, Z. Qu, M.W. Bidez, Mechanical properties of trabecular bone in the human mandible: implications for dental implant treatment planning and surgical placement, J. Oral Maxillofac. Surg. 57 (6) (1999) 706–708 https://doi.org/10.1016/S0278-2391(99)90437-8.
[32] S.K. Pandey, C. Haldar, D.K. Vishwas, P. Maiti, Synthesis and in vitro evaluation of melatonin entrapped PLA nanoparticles: an oxidative stress and T-cell response using golden hamster, J. Biomed. Mater. Res. A. 103 (9) (2015) 3034–3044 https://doi.org/10.1002/jbm.a.35441.
[33] N. Passerini, D.Q.M. Craig, An investigation into the effects of residual water on the glass transition temperature of polylactide microspheres using modulated temperature DSC, J. Control. Release 73 (2001) 111–115 https://doi.org/10.1016/S0168-3659(01)00245-0.
[34] O.J. Karlsson, J.M. Stubbs, L.E. Karlsson, D.C. Sundberg, Estimating diffusion coefficients for small molecules in polymers and polymer solutions, Polymer 42 (2001) 4915–4923 https://doi.org/10.1016/S0032-3861(00)00765-5.
[35] J.L. Calvo-Guirado, G. Gomez-Moreno, J.E. Mate-Sanchez, L. Lopez-Mari, R. Delgado-Ruiz, G.E. Romanos, New bone formation in bone defects after melatonin and porcine bone grafts: experimental study in rabbits, Clin. Oral Implant. Res. 26 (4) (2015) 399–406 https://doi.org/10.1111/clr.12364.
[36] K. Zwirska-Korczala, J. Jochem, M. Adamczyk-Sowa, P. Sowa, R. Polaniak, E. Birkner, M. Latocha, K. Pilc, R. Suchanek, Influence of melatonin on cell proliferation, antioxidative enzyme activities and lipid peroxidation in 3T3-L1 preadipocytes–an in vitro study, J. Physiol. Pharmacol. 56 (6) (2005) 91–99.
[37] I. Manjubala, A. Woesz, C. Pilz, M. Rumpler, N. Fratzl-Zelman, P. Roschger, J. Stampfl, P. Fratzl, Biomimetic mineral-organic composite scaffolds with controlled internal architecture, J. Mater. Sci. Mater. Med. 16 (12) (2005) 1111–1119 https://doi.org/10.1007/s10856-005-4715-6.
[38] J.A. Roth, B.G. Kim, W.L. Lin, M.I. Cho, Melatonin promotes osteoblast differentiation and bone formation, J. Biol. Chem. 274 (31) (1999) 22041–22047 https://doi.org/10.1074/jbc.274.31.22041.
[39] N.I. zur Nieden, G. Kempka, H.J. Ahr, In vitro differentiation of embryonic stem cells into mineralized osteoblasts, Differentiation 71 (1) (2003) 18–27 https://doi.org/10.1046/j.1432-0436.2003.700602.x.